

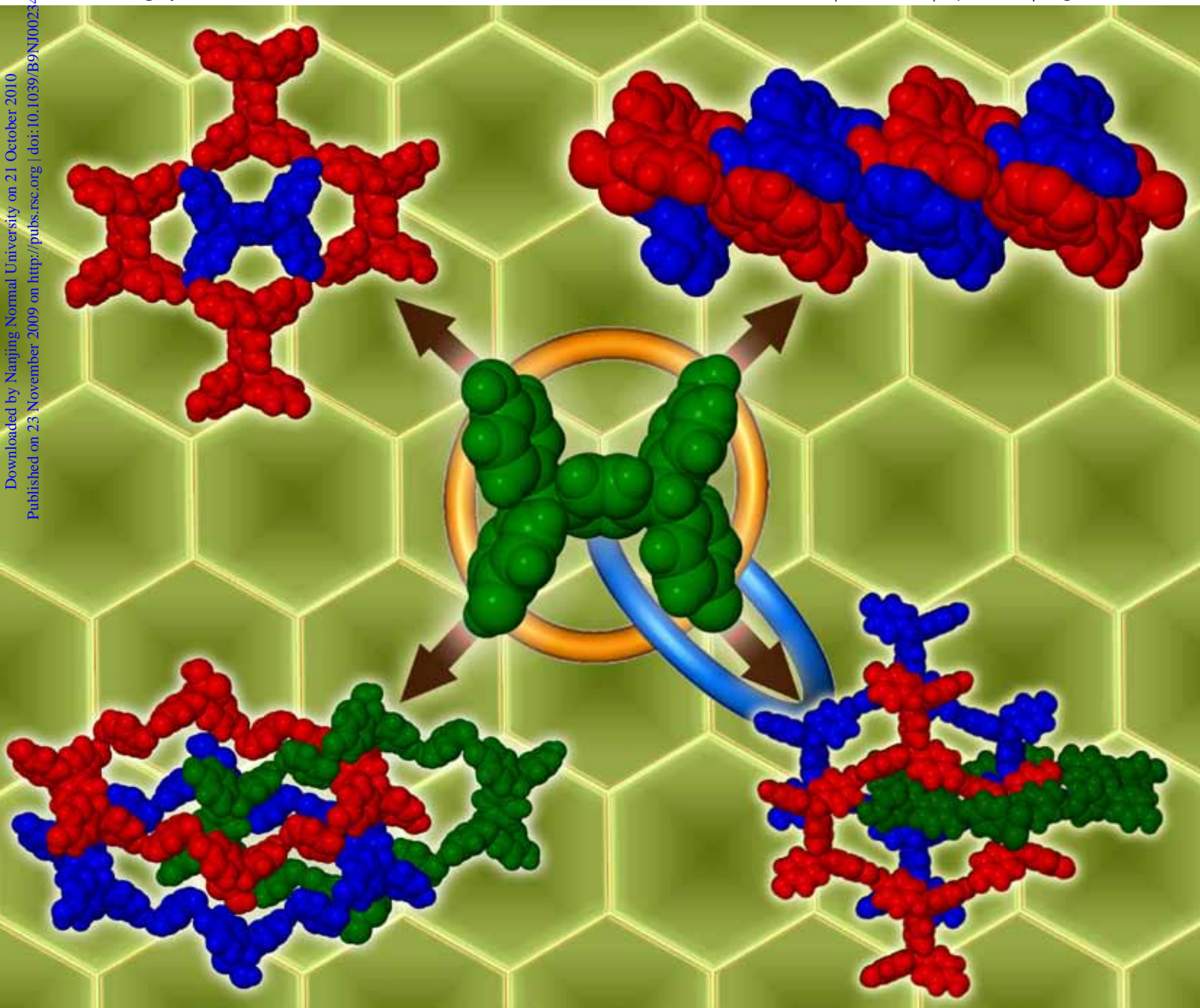
# NJC

New Journal of Chemistry

An international journal of the chemical sciences

[www.rsc.org/njc](http://www.rsc.org/njc)

Volume 34 | Number 4 | April 2010 | Pages 573–768

Downloaded by Nanjing Normal University on 21 October 2010  
Published on 23 November 2009 on <http://pubs.rsc.org> | doi:10.1039/B9NJ00244K

ISSN 1144-0546

RSC Publishing



**PAPER**  
Ashwini Nangia *et al.*  
Supramolecular networks of a  
H-shaped aromatic phenol host



1144-0546(2010)34:4;1-O

# Supramolecular networks of a H-shaped aromatic phenol host†

Ranjit Thakuria, Bipul Sarma and Ashwini Nangia\*

Received (in Montpellier, France) 2nd June 2009, Accepted 5th October 2009

First published as an Advance Article on the web 23rd November 2009

DOI: 10.1039/b9nj00234k

X-Ray crystal structures of 1,4-di[bis(hydroxyphenyl)methyl]benzene and its solvates and cocrystals were analyzed for the occurrence of network architectures. From the simplest 1D ladder in EtOAc, DMSO and *i*-PrOH solvates of **1** ( $R_1 = R_2 = R_4 = \text{H}$ ,  $R_3 = \text{OH}$ ), doubly-interpenetrated 1D ladders in its guest-free form and 1D/2D-interpenetrated ladder networks in a cocrystal with phenazine were identified. The dioxane and DMSO solvates of **2** ( $R_1 = R_3 = \text{OMe}$ ,  $R_2 = \text{OH}$ ,  $R_4 = \text{H}$ ), and the DMSO and toluene solvates of **4** ( $R_1 = \text{H}$ ,  $R_2 = R_4 = \text{Me}$ ,  $R_3 = \text{OH}$ ) also adopt 1D ladder networks. Monomethyl phenol **3** ( $R_1 = R_2 = \text{H}$ ,  $R_3 = \text{OH}$ ,  $R_4 = \text{Me}$ ) makes 2D grids of ladders that include nitromethane solvent in the channels. The hexagonal (6,3) net in the cocrystal of **1** with pyrazine-*N,N'*-dioxide is triply-interpenetrated in a 2D architecture. The DMF solvate of **3** is similar to **1**·(PyzNO)<sub>2</sub>, except that the (6,3) nets are doubly-interpenetrated *via* Hopf links. An orthorhombic nitromethane solvate of **1** is 2D → 3D polycatenated with a degree of catenation (DOC) = 2/2, whereas the monoclinic polymorph of **1**·(CH<sub>3</sub>NO<sub>2</sub>)<sub>2</sub>, as well as the chloroform inclusion structure of **4**, adopt the rare (5,3) pentagonal net. Platonic (6,3) and Catalan (5,3) nets in the broader category of a uniform network topology were realized from H-shaped molecules **1–4** in different solvent inclusion and cocrystal structures. Finally, a cocrystal of **1** with quinoxaline forms a polyrotaxane 1D → 1D chain of Euclidean entanglement. Polythreaded rotaxane, pentagonal Catalan and 1D/2D interpenetrated nets are, as such, rare in organic molecular crystals. The role of the solvent/co-former in affording diverse supramolecular networks and entanglement modes are rationalized in the crystal structures.

## Introduction

Network architectures are common in inorganic structures, minerals, metal–organic compounds and coordination polymers.<sup>1</sup> Robson, Batten, Ciani, Carlucci and Proserpio have reviewed<sup>2</sup> recent examples of polycatenation, polythreading and polyknotting in coordination structures. Carlucci *et al.*<sup>3</sup> distinguished interpenetration from catenation, in that the former type of entanglement involves no change in the dimensionality of the original 2D or 3D nets, whereas the latter entanglement type increases the overall dimensionality of 1D or 2D components to a higher level. In contrast, Batten and Robson<sup>1c,2c</sup> refer to both situations as interpenetration, albeit of different types.

In general, the classification of organic crystal structures as nets is a recent and less common trend; the similarity of the rhombohedral hydroquinone structure ( $\beta$ -polymorph) to  $\beta$ -polonium being a classic example. The fact that hydrogen bonds are weaker and less directional than metal–heteroatom and metal–ligand bonds means that the geometry of organic structures is not as clearly definable as that at the metal center of coordination compounds and polymers. Even though hydrogen bond directionality has an angular spread, organic

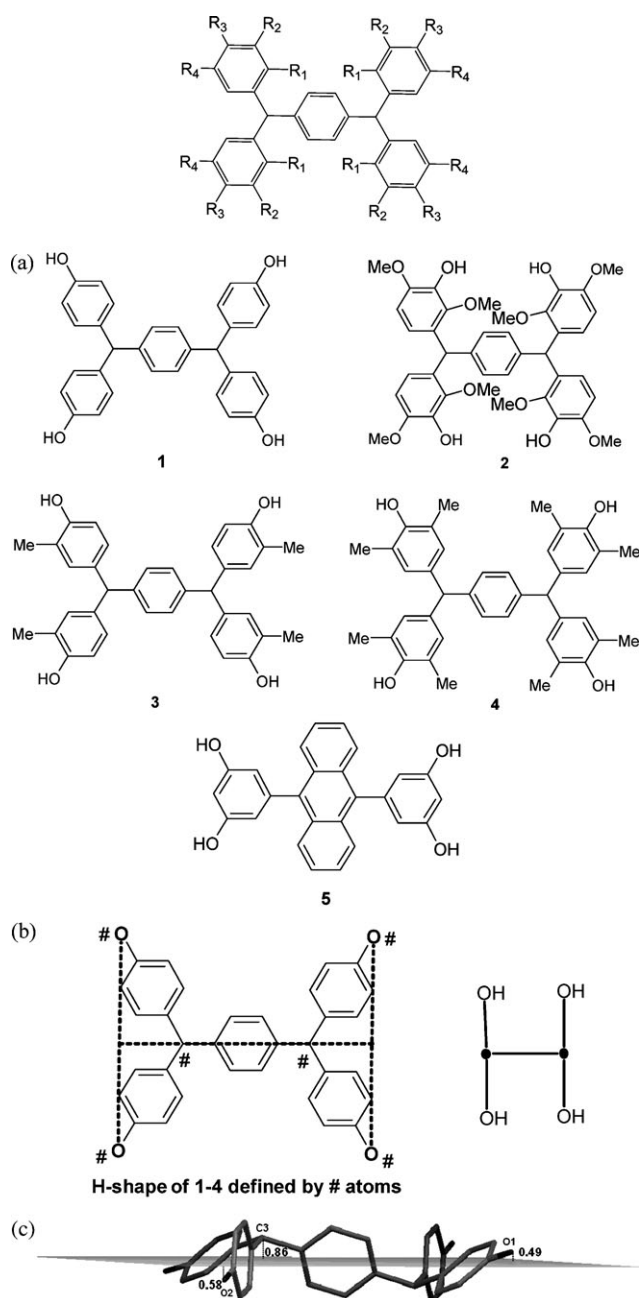
crystal structures can be topologically classified akin to inorganic and coordination network structures.<sup>1d,1e,1h,4</sup> Recent literature<sup>1,2,4</sup> indicates that the number and diversity of network topologies in organic structures is not as prolific compared to those formed in metal–organic coordination polymers. The classification of crystal structures as networks is a first step to establishing topological similarities between architectures built from organic, inorganic or metal–organic building units, which is an important activity in crystal engineering, with applications in materials science. Here, we present new examples of rare network topologies and interpenetration/catenation modes of organic supramolecular architectures built from a H-shaped tecton.

## Results

1,4-Di[bis(4'-hydroxyphenyl)methyl]benzene (**1**) and its methoxy and methyl derivatives **2–4** were prepared by the acid-catalyzed condensation of terephthalaldehyde with the requisite phenol (4 equiv.).<sup>5</sup> All compounds were purified and characterized by their NMR and IR spectra. These molecules may be viewed as having a *para*-substituted phenyl linker that connects bis(hydroxyphenyl)methyl groups on the two sides for directed self-assembly (Fig. 1(a)). The peripheral O atoms that engage in hydrogen bonding and their connectivity to the carbon core *via* tetrahedral C atoms are considered to define the H-shape of prototype molecule **1**. The fact that the connecting carbon centers are sp<sup>2</sup> or sp<sup>3</sup> hybridized and have angles that are far from the idealized 180° and 90° is not

School of Chemistry, University of Hyderabad, Hyderabad 500 046, India. E-mail: ashwini.nangia@gmail.com

† Electronic supplementary information (ESI) available: Crystal packing diagrams and DSC/TGA plots. CCDC reference numbers 717784–717798. For crystallographic data in CIF or other electronic format see DOI: 10.1039/b9nj00234k



**Fig. 1** (a) Molecules 1–4 used for network construction in this paper. The phenol OH groups are oriented outward to form hydrogen bond networks. (b) The H-shape of the molecular core of **1** is realized by connecting the phenol O atoms and the central *para*-phenyl linker C atoms. (c) The # atoms that make up the H-shape are nearly coplanar, deviating from the mean plane by 0.49, 0.58 and 0.86 Å. Molecule **1** is extracted from its MeOH solvate structure (ref. 5).

relevant. What is important is that the mean plane of the phenol O and *para*-phenyl linker C atoms (marked # in Fig. 1(b)) are nearly coplanar (Fig. 1(c), deviation from the mean plane < 1 Å) and make an idealized H-shape. The importance of tetraphenol hosts was emphasized by Aoyama's group as a new class of organic zeolites in the inclusion structures of **5** and its derivatives.<sup>6</sup> H-shaped organic molecular tectons are, as such, rare to our knowledge, even though there are examples of

Y- and T-shaped organic tectons,<sup>1e,1i,1j,4,7</sup> L-shaped<sup>8</sup> molecules, and V-shaped<sup>9</sup> molecular tweezers. The significant literature on metal–ligand building blocks for assembling supramolecular networks of coordination compounds and infinite polymers, which is somewhat outside the scope of this article, is reviewed elsewhere.<sup>1e,1g,2,10</sup> H-shaped organic pentiptycene functional molecules<sup>11a</sup> and an Mo–Au phosphinidene complex<sup>11b</sup> are known, but these structures are not in the host–guest or co-crystal network category. H-shaped tetraphenol host **1** is, as such, a new tecton in organic nets with only two short papers having been published by our group.<sup>5,12</sup> Here, we present network diversity in the solvates and co-crystals of **1–4**. When the guest species is a typical solvent, the binary adduct is referred to as a solvate, and if the second component is a solid co-former then the product is generally called a co-crystal. Although “solvate” and “co-crystal” have slightly different meanings, both terms are used within the broader category of multi-component crystal structures.<sup>13</sup> Network structures are described in the order of 1D ladders<sup>6a,14</sup> to interpenetrated ladders to 2D hexagonal sheets<sup>15</sup> to polycatenated 3D frameworks to Catalan ( $5_3^2$ )<sup>12</sup> and polyrotaxane<sup>16</sup> nets.

Crystallization of **1** from EtOAc gave solvated crystal **1**·(EtOAc)<sub>2</sub> in the space group  $P\bar{1}$  with half a molecule of **1** in the crystallographic unit due to the imposed inversion symmetry. The host molecules form a 1D ladder network through phenol O–H···O hydrogen bonds (O1–H1···O2 1.78 Å, 165°; Table 1) and the EtOAc molecules are connected on the sides (O2–H2A···O4 1.75 Å, 173°). Adjacent layers of host and guest molecules are offset in such a way that the ladder rung region (cavity dimensions are given in Table 2) is sandwiched between guest molecules of adjacent layers. In **1**·(DMSO)<sub>2</sub> solvate (monoclinic space group  $P2_1/c$ , half molecule of **1**), the solvent molecule acts as a connector to convergently direct OH groups of the host *via* O–H···O hydrogen bonds (O2–H2A···O3, 1.74 Å, 171°; O1–H1A···O3, 1.69 Å, 172°). The difference in the O–H···O bonds between the two structures (Fig. 2) is attributed to the stronger hydrogen bond acceptor basicity of DMSO compared to EtOAc (p*K*<sub>HB</sub> scale: S=O 2.58, C=O 1.00).<sup>17</sup> DMSO acts as a dual acceptor of hydrogen bonds from two host molecules and becomes part of the ladder network, whereas EtOAc is a single hydrogen bond acceptor from the host ladder. The *i*-PrOH solvate **1**·(*i*-PrOH)<sub>4</sub> (p*K*<sub>HB</sub> O<sub>sp</sub><sup>3</sup> 0.82) is similar to the EtOAc structure. However, a difference between the EtOAc and *i*-PrOH solvent molecules is that the former behaves as a terminal acceptor whereas the latter is a connector of host ladder nets *via* helical O–H···O trimers (Fig. S1, ESI†). There is a half molecule of **1** and two *i*-PrOH molecules in the unit cell of **1**·(*i*-PrOH)<sub>4</sub>, of which one disordered guest molecule was removed using the SQUEEZE program (see the Experimental section). Small solvent molecules reside in the ladder rung regions to give a close-packed crystal structure (see Fig. S2 for more examples, ESI†).

A half molecule of **1–4** is present in the unit cell of solvates, co-crystals and guest-free forms that crystallize in space groups with an inversion center, the only exception being the **1**·(4,4'-BipyNO)<sub>2</sub> co-crystal with the space group  $Pca2_1$ . Octamethoxy derivative **2** gave crystalline solvate **2**·(dioxane)<sub>2</sub> with the space group  $P\bar{1}$ , whose 1D ladder network is structurally similar to

**Table 1** Hydrogen bonds in the crystal structures of **1–4**

Compound	Interaction	H...A/Å	D...A/Å	D-H...A (°)	Symmetry code
<b>1</b>	O1–H1A...O3	1.76	2.729(4)	168	1 - x, 2 - y, 1 - z
	O2–H2A...O1	1.82	2.789(4)	167	x, -1 + y, z
	O3–H3A...O4	1.72	2.683(5)	165	x, 1 + y, z
	C16–H16...O2	2.45	3.512(5)	167	1 - x, 1 - y, -z
<b>1·(DMSO)<sub>2</sub></b>	C22–H22...O2	2.46	3.389(5)	143	-1 + x, y, z
	O1–H1A...O3	1.69	2.663(3)	172	1 + x, -1 + y, z
	O2–H2A...O3	1.74	2.711(3)	171	x, -1 + y, z
<b>1·(EtOAc)<sub>2</sub></b>	C18–H18A...O2	2.32	3.400(6)	173	-x, ½ + y, ½ - z
	O1–H1...O2	1.78	2.742(1)	165	x, y, 1 + z
	O2–H2A...O4	1.75	2.725(1)	173	1 - x, 1 - y, -z
<b>1·(i-PrOH)<sub>4</sub></b>	C16–H16...O3	2.36	3.426(2)	166	— <sup>a</sup>
	O1–H1...O2	1.66	2.629(3)	167	x, -y, -½ + z
	O2–H2A...O3	1.61	2.588(3)	171	x, 1 - y, ½ + z
<b>1·(4,4'-BipyNO)<sub>2</sub></b>	O3–H3A...O1	1.74	2.715(3)	170	— <sup>a</sup>
	O1–H1A...O5	1.64	2.611(8)	169	x, -1 + y, z
	O2–H2A...O6	1.64	2.423(11)	133	-x, -y, -½ + z
	O3–H3A...O8	1.71	2.682(8)	168	½ - x, 1 + y, -½ + z
	O4–H4A...O7	1.84	2.641(8)	136	x, 1 + y, z
	C37–H37...O6	2.43	3.513(11)	179	½ + x, 1 - y, z
	C52–H52...O7	2.41	3.478(11)	168	½ + x, -y, z
<b>1·(Phez)<sub>1.5</sub></b>	O1–H1A...O2	1.81	2.791(3)	179	x, -1 + y, z
	O2–H2A...N2	1.78	2.739(3)	166	1 + x, 1 + y, z
	O3–H3A...N1	1.99	2.950(4)	165	— <sup>a</sup>
	O4–H4...O3	1.92	2.848(3)	156	x, -1 + y, z
	C43–H43...O4	2.33	3.353(7)	157	1 - x, -y, 1 - z
<b>1·(PyzNO)<sub>2</sub></b>	O1–H1A...O4	1.72	2.669(2)	161	1 + x, 1 + y, z
	O2–H2A...O3	1.78	2.757(3)	170	x, ¾ - y, -½ + z
	C19–H19...O2	2.30	3.328(3)	157	-x, -½ + y, ½ - z
	C20–H20...O1	2.23	3.283(3)	164	-1 + x, ¾ - y, ½ + z
<b>1·(Quinox)<sub>2</sub></b>	O1–H1A...N1	1.86	2.826(4)	169	1 + x, y, -1 + z
	O2–H2A...N2	1.84	2.816(4)	173	1 - x, -y, -z
	C22–H22...O2	2.40	3.477(5)	172	x, ½ - y, ½ + z
	O2–H2...O5	1.94	2.880(5)	159	x, -1 + y, z
<b>2·(dioxane)<sub>2</sub></b>	O5–H5...O7	2.06	2.867(5)	138	— <sup>a</sup>
	C19–H19B...O1	2.49	3.404(6)	142	1 - x, 1 - y, -z
	C20–H20B...O6	2.49	3.350(6)	135	1 - x, 2 - y, 1 - z
	O2–H2...O5	1.96	2.744(3)	135	1 + x, y, z
	O5–H3...O7	1.72	2.653(4)	156	-1 + x, y, -1 + z
<b>2·(DMSO)<sub>2</sub></b>	C6–H6...O4	2.36	3.387(4)	157	1 + x, ¾ - y, ½ + z
	C21–H21C...O3	2.43	3.355(5)	142	x, y, 1 + z
	O1–H1A...O2	1.77	2.750(3)	176	½ + x, ¾ - y, ½ + z
	C13–H13...O1	2.40	3.365(3)	148	½ - x, ½ + y, ¾ - z
<b>3·(CH<sub>3</sub>NO<sub>2</sub>)<sub>2</sub></b>	O1–H1A...O2	1.75	2.724(3)	171	1 - x, -y, -z
	O2–H2A...O1	1.87	2.789(3)	155	x, -1 + y, z
<b>4</b>	O1–H1...O1	2.33	3.267(3)	158	-x, -½ + y, ½ - z
	O1–H1...O3	1.80	2.723(5)	155	-1 + x, 1 + y, z
<b>4·(DMSO)<sub>2</sub></b>	O2–H2...O1	1.96	2.875(6)	155	1 + x, y, z
	C17–H17A...O2	2.40	3.280(7)	137	-1 + x, y, z
	C18–H18C...O3	2.47	3.233(7)	126	-1 + x, 1 + y, z
	C22–H22A...O3	2.44	3.476(7)	159	2 - x, -y, -z
	O2–H2...O1	2.06	2.935(3)	147	x, 1 + y, -1 + z

<sup>a</sup> Host...guest interaction.

**1·(EtOAc)<sub>2</sub>**. Adjacent ladders are connected *via* dioxane (O5–H5...O7 2.06 Å, 138°) to give a 2D sheet structure. A second guest molecule (O8 dioxane) fills the space in the channel framework (Fig. 3(a)). There are two crystallographically distinct solvent molecules, both residing on inversion centers: O7 and O8 dioxane molecules are disordered over two positions, with disorder being modelled in both cases. Compound **3**, on crystallization from nitromethane, afforded a host ladder network structure (Fig. 3(b)) similar to the **4·(CH<sub>3</sub>NO<sub>2</sub>)<sub>2</sub>** solvate, which extends into a 2D sheet through O–H...O hydrogen bonds. A guest-free form of **4** was crystallized from dichloromethane, but this crystal structure (Fig. S3, ESI<sup>†</sup>) cannot be classified as a net.

A guest-free form of **1** was obtained upon crystallization from CH<sub>3</sub>NO<sub>2</sub> in the space group *P* $\bar{1}$  with two half molecules in the asymmetric unit (*Z'* = 2), a situation that arises in crystal structures where the molecule has a packing problem.<sup>7a,18</sup> 1D ladder networks sustained by O–H...O hydrogen bonds (O1–H1A...O3, 1.76 Å, 168°; O2–H2A...O1, 1.82 Å, 167°; O3–H3A...O4, 1.72 Å, 165°) run along [010]. Two such networks are inclined at an angle of 73.6° and interpenetrate such that the *para*-phenyl connectors of the second ladder weave through the rectangular rungs of the first (Fig. 4).

Compound **1** and phenazine (Phez) afforded cocrystal **1·(Phez)<sub>1.5</sub>**, with one full and one half molecule of phenazine and two half molecules of **1** in the unit cell (*P* $\bar{1}$ ). One of the

**Table 2** Network classification and description



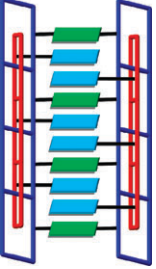
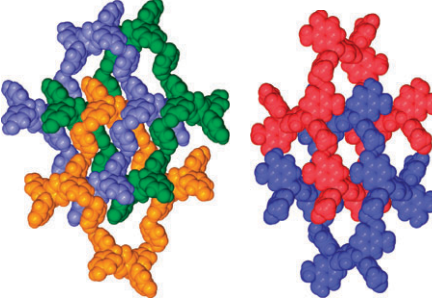
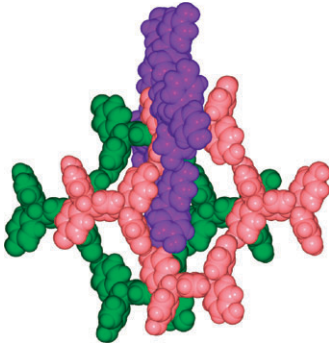

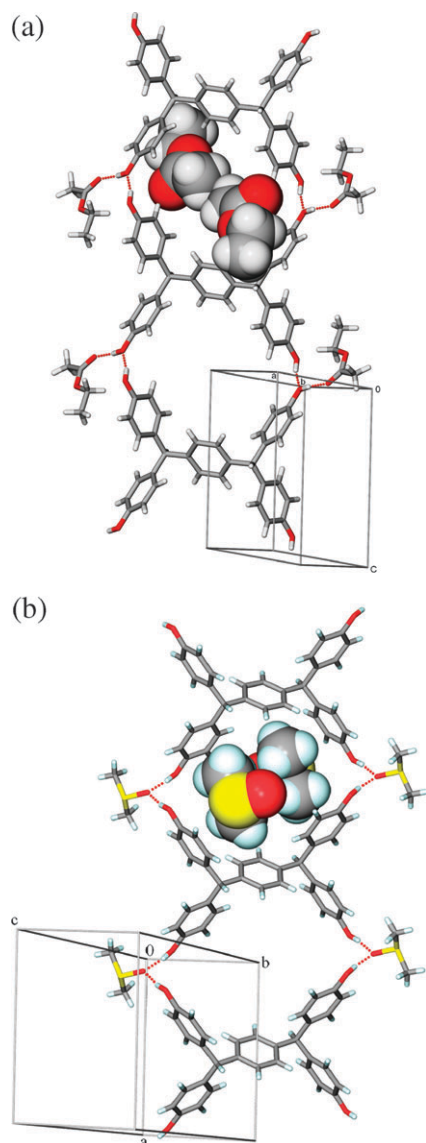
Network type	Network graphic	Crystal structure	Ladder rung dimensions (Ph ring centroid to centroid)/Å	Ladder rung dimensions (actual distance after removing vdW radius)/Å	Network description
1D ladder with guest inclusion		1-(EtOAc) <sub>2</sub> 1-(DMSO) <sub>2</sub> 1-(i-PrOH) <sub>4</sub> 1-(dioxane) <sub>2</sub> <sup>5</sup> 1-(CH <sub>3</sub> CN) <sub>2</sub> <sup>5</sup> 1-(4,4'-Bipy) <sub>2</sub> <sup>5</sup> 2-(dioxane) <sub>2</sub> 2-(DMSO) <sub>2</sub> 3-(CH <sub>3</sub> NO <sub>2</sub> ) <sub>2</sub> <sup>12</sup> 4-(CH <sub>3</sub> NO <sub>2</sub> ) <sub>2</sub> <sup>12</sup> 4-(DMSO) <sub>2</sub> 4-(toluene) 4-(CH <sub>3</sub> CN) <sub>2</sub> <sup>5</sup>	7.9 × 6.8 <sup>a</sup> 8.7 × 5.9 <sup>a</sup> 7.5 × 5.1 <sup>a</sup> 7.8 × 6.9 7.8 × 6.5 16.7 × 6.9 13.5 × 7.6 <sup>b</sup> 9.2 × 8.4 <sup>b</sup> 8.5 × 7.0 <sup>a</sup> 8.6 × 8.0 <sup>a</sup> 7.8 × 6.8 <sup>a</sup> 8.2 × 7.1 <sup>a</sup> 8.7 × 7.2	6.3 × 5.1 <sup>a</sup> 8.7 × 5.2 <sup>a</sup> 4.4 × 4.9 <sup>a</sup> 7.6 × 4.9 7.8 × 4.0 16.7 × 6.9 No cavity <sup>b</sup> No cavity <sup>b</sup> 8.2 × 3.7 <sup>a</sup> 5.1 × 7.9 <sup>a</sup> 7.7 × 6.4 <sup>a</sup> 8.2 × 6.4 <sup>a</sup> 8.4 × 4.7	1D ladder with a cavity for guest inclusion between the rungs <sup>a</sup> or between the ladders <sup>b</sup>
1D → 1D interpenetration		1 (guest-free)	7.9 × 6.6	6.6 × 5.1	Ladders interpenetrate at 73.6° and are connected by hydrogen bonds in the 3D structure
1D/2D interpenetration		1-(Phez) <sub>1,5</sub>	7.7 × 6.1	6.9 × 4.7	One host ladder and a Phez connector form a 2D sheet that is interpenetrated by the second ladder at 73°; the latter ladder has dangling Phez molecules
2D → 2D interpenetration		1-(PyzNO) <sub>2</sub>	25.1 × 14.1 × 11.8 <sup>c</sup>	22.2 × 14.1 × 8.4 <sup>c</sup>	Three-fold interpenetration of (6,3) nets to give 2D layers. A PyzNO spacer increases the cavity size to give triple interpenetration <i>via</i> a Hopf link
		3-(DMF) <sub>2</sub>	20.1 × 7.1 × 7.1 <sup>c</sup>	19.1 × 8.1 × 4.0 <sup>c</sup>	Doubly interpenetrated (6,3) net. The cavity dimensions are smaller than in the PyzNO cocrystal

Table 2 (continued)

Network type	Network graphic	Crystal structure	Ladder rung dimensions (Ph ring centroid to centroid)/Å	Ladder rung dimensions (actual distance after removing vdW radius)/Å	Network description
Polycatenation 2D → 3D		1-(CH <sub>3</sub> NO <sub>2</sub> ) <sub>2</sub> <i>Pbca</i> form <sup>12</sup> 1-(CH <sub>3</sub> OH) <sub>2</sub> <sup>5</sup> 1-(C <sub>2</sub> H <sub>5</sub> OH) <sub>2</sub> <sup>5</sup>	18.6 × 13.3 × 11.9 <sup>c</sup> 18.4 × 11.8 × 12.6 <sup>c</sup> 18.9 × 11.8 × 12.7 <sup>c</sup>	18.6 × 13.3 × 10.3 <sup>c</sup> 18.4 × 10.5 × 12.6 <sup>c</sup> 18.9 × 10.6 × 12.7 <sup>c</sup>	DOC = 2/2, which means two parallel layers are catenated with one hexagonal ring and <i>vice versa</i> . A difference between 1-(PyzNO) <sub>2</sub> and these structures is that both have a Hopf link, but in the PyzNO co-crystal, all three (6,3) nets are in the same plane (no change in dimensionality) and to remove any one net a bond must be broken. The dimensionality in the CH <sub>3</sub> NO <sub>2</sub> solvate increases from 2D → 3D and two parallel (6,3) nets not connected by a Hopf link weave through the third net
Catalan or (5,3) net		1-(CH <sub>3</sub> NO <sub>2</sub> ) <sub>2</sub> <i>P2<sub>1</sub>/c</i> form <sup>12</sup> 4-(CHCl <sub>3</sub> ) <sub>2</sub> <sup>12</sup>	5.6 × 4.9 5.7 × 5.5	5.6 × 4.5 5.4 × 5.4	The pentagonal sheet is flat for the 4 solvate but a 3D 3,4-connected net in the 1 solvate. There are three 3-connected and two 4-connected nodes in each pentagon
Polythreading or polyrotaxane (Euclidean entanglement)		1-(Quinox) <sub>2</sub>	8.6 × 8.0 × 6.3 <sup>c</sup>	7.0 × 5.4 × 4.7 <sup>c</sup>	The 1D chain motif is comprised of alternating rings and rods to make the polyrotaxane. This motif is common in metal-organic frameworks

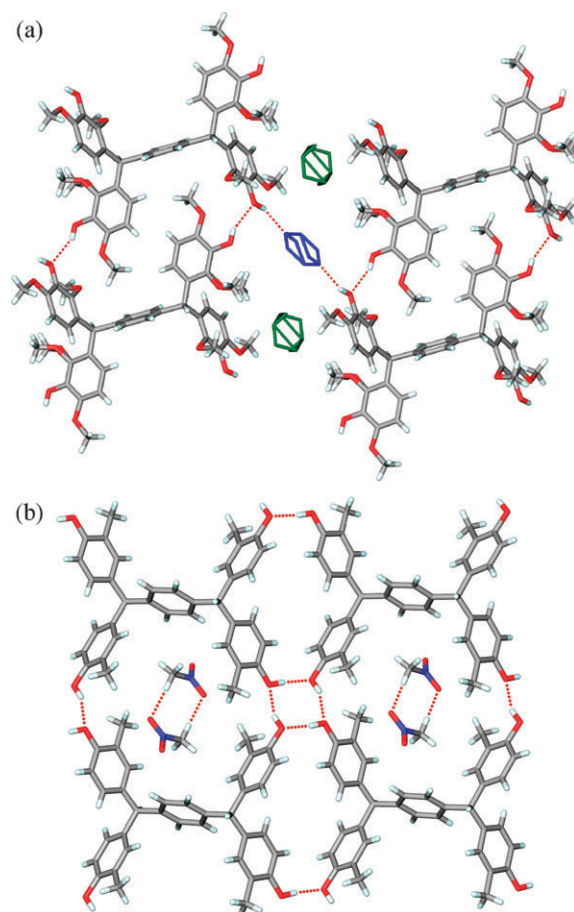
<sup>a</sup> Cavity between ladder rungs. <sup>b</sup> Cavity in ladder's connector region. <sup>c</sup> The three sides of the pseudohexagonal cavity have slightly different dimensions.



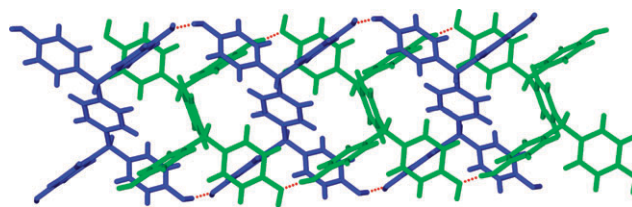
**Fig. 2** (a) The host ladder network of **1** along [001]. EtOAc molecules are hydrogen-bonded on the sides and lie above/below the rung region of adjacent layer ladders. (b) The DMSO solvate of **1**. Solvent molecules connect H-shaped phenols via O–H...O hydrogen bonds in a host-guest ladder network along [100].

host molecules (blue in Fig. 5) together with a half Phez (green) molecule form a 2D sheet sustained by O–H...O and O–H...N hydrogen bonds (O4–H4...O3 1.92 Å, 156°; O3–H3A...N1 1.99 Å, 165°). The second ladder (red) weaves through the rectangular rung regions of the first ladder, which is part of the 2D sheet, at an inclination of 73° to give a rare example of a 1D/2D interpenetrated network. The second Phez (light blue) molecule dangles from the (red) second ladder (O1–H1A...O2 1.81 Å, 179°; O2–H2A...N1 1.78 Å, 166°) and does not act as a connector.

The crystal structure of **1** with 4,4'-bipyridine,<sup>5</sup> **1**-(4,4'-Bipy)<sub>2</sub>, forms a perfect 1D ladder network (Fig. 6(a)). This structure is comparable with the 4,4'-bipyridine-*N,N'*-dioxide (4,4'-BipyNO) cocrystal of **1** (Fig. 6(b)). Whereas geometrically the co-former is a linear extension upon going from



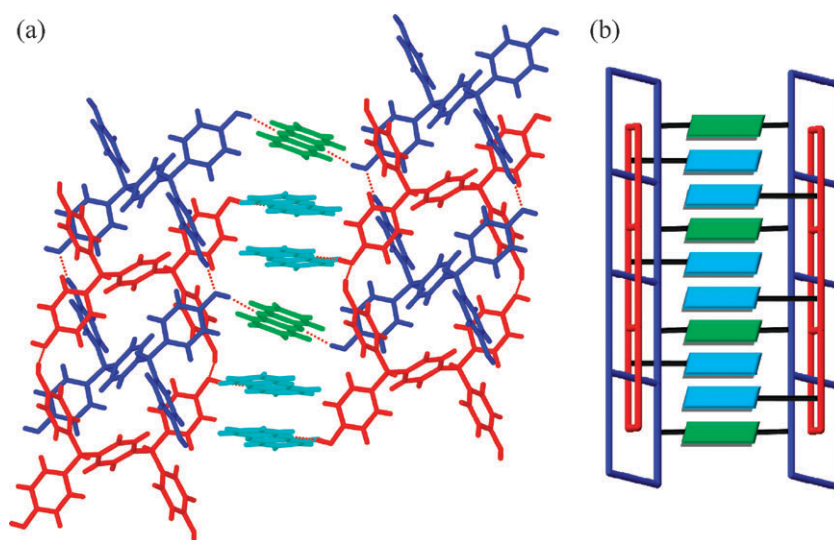
**Fig. 3** (a) The host ladder network of **2** is connected by dioxane (O7, blue) and filled with a second dioxane molecule in the channels (O8, green) of the **2**-(dioxane)<sub>2</sub> solvate. Methoxy groups self-include in the rung region. (b) The crystal structure of **3**-(CH<sub>3</sub>NO<sub>2</sub>)<sub>2</sub> showing the cooperative O–H...O hydrogen bond tetramer that assembles and connects 1D ladder networks and nitromethane C–H...O dimers in the rectangular rungs.



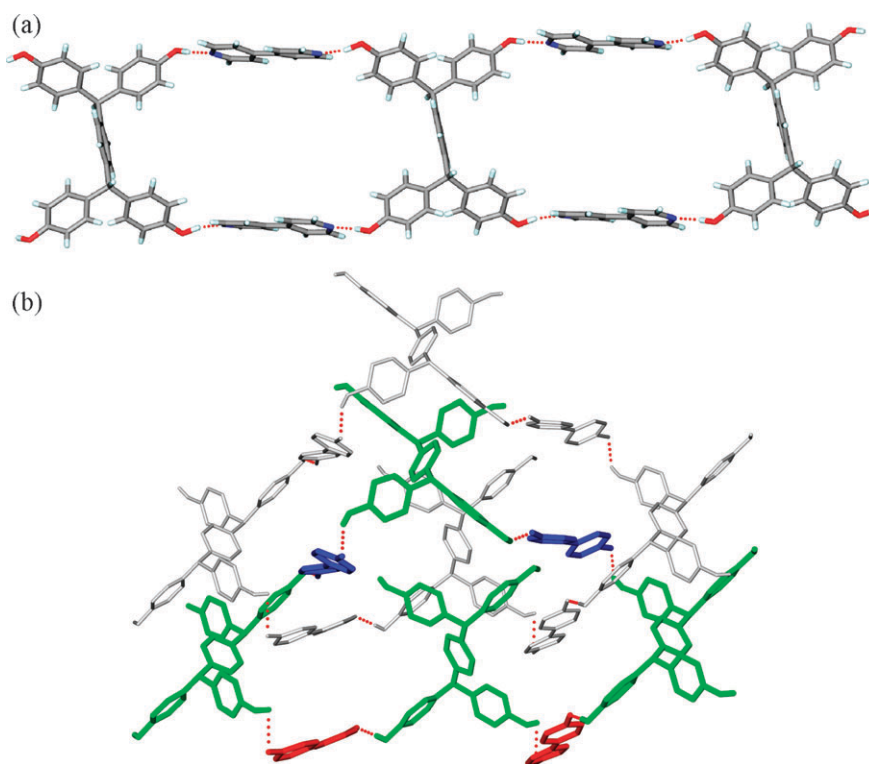
**Fig. 4** Double interpenetration of inclined ladders in the guest-free form of **1**. Symmetry-independent molecules are colored differently.

pyridine to pyridine-*N*-oxide, the corresponding cocrystal structures are very different. The latter structure is topologically a (6,3) net, where 4,4'-BipyNO expands the ring size and is filled, in part, by self-inclusion of the H-shaped molecule.

With DMF solvent, **3** produced a structure having disordered solvent molecules that were removed using the SQUEEZE program (see Experimental section). **3**-(DMF)<sub>2</sub> is an example of a 2D → 2D interpenetration of (6,3) honeycomb nets. Here, the hexagonal net is expanded in 2D and another (6,3) net is intertwined in a parallel fashion (Fig. 7(a)), illustrating a clear case of interpenetration through Hopf links



**Fig. 5** Interpenetrated ladders in the  $1\text{-(Phez)}_{1.5}$  cocrystal. (a) Phez and host molecules (green and blue) form a 2D sheet that is interpenetrated by a host ladder (red) with dangling Phez molecules (light blue). (b) The 1D/2D interpenetrated ladder network in the same color scheme as (a).



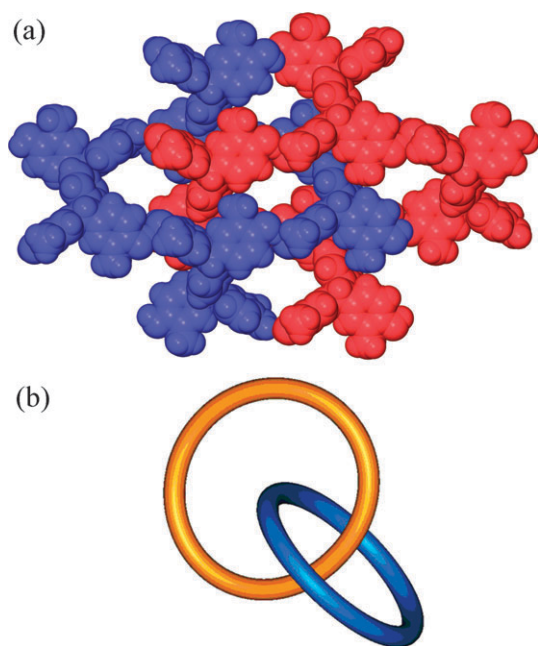
**Fig. 6** (a) Hydrogen-bonded ladders in  $1\text{-(4,4'-Bipy)}_2$  with rectangular rung dimensions of  $16.7 \times 6.9 \text{ \AA}$ . No solvent is included in the crystal lattice. Close packing is achieved by the offset stacking of ladders (ref. 5). (b)  $1\text{-(4,4'-BipyNO)}_2$  is topologically a (6,3) net of host molecule self-inclusion. The arrangement of the pendant groups is inside the supramolecular ring for one of the H-shaped molecules, leading to partial self-inclusion. This structure is not easily classified as a net. Molecular rings overlay as shown.

(Fig. 7(b)). These can be defined as two-component links of two unknots that no isotopy can separate, such that there are two non-intersecting spheres that can isolate each component, or simply two interlocked rings that can be separated only by cutting open one ring.

In the cocrystal of **1** with pyrazine-*N,N'*-dioxide,  $1\text{-(PyzNO)}_2$ , the host molecule is hydrogen-bonded to the

*N*-oxide O acceptor in a (6,3) network. Due to the tetrahedral angle at the OH donor group and the bent hydrogen bond to the PyzNO spacer (O1–H1A...O4  $1.72 \text{ \AA}$ ,  $161^\circ$ ; O2–H2A...O3  $1.78 \text{ \AA}$ ,  $170^\circ$ ), the ring size of the (6,3) topological net is actually an expanded 6-membered ring. A single ring of  $22.2 \times 14.1 \times 8.4 \text{ \AA}$  (dimensions in Table 2 give the available space inside) is occupied by two identical rings to



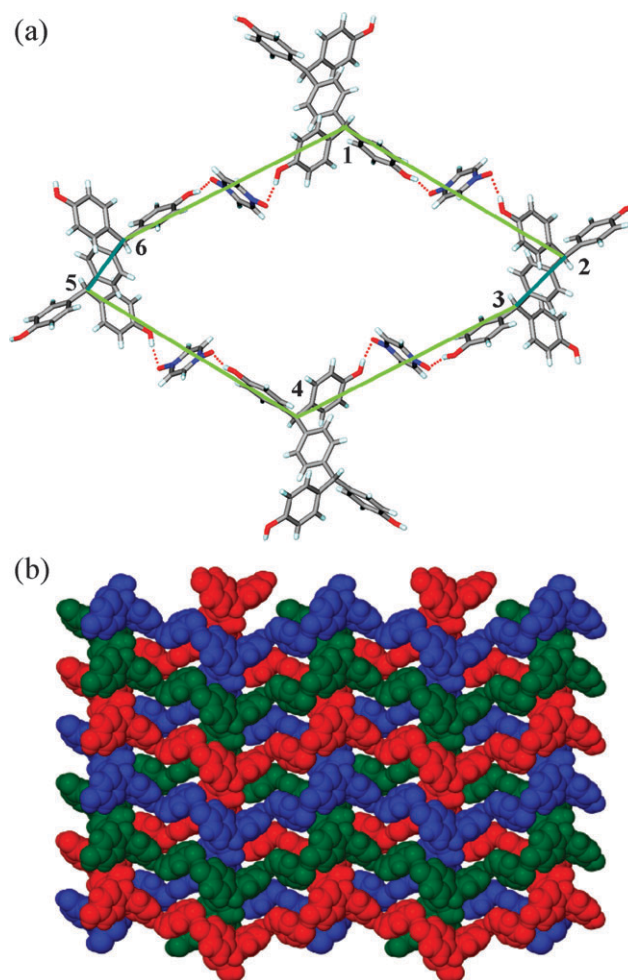


**Fig. 7** (a) Parallel 2D  $\rightarrow$  2D 2-fold interpenetration in the crystal structure of  $3\cdot(\text{DMF})_2$ . Disordered solvent molecules are omitted. (b) A Hopf link.

give a 2D  $\rightarrow$  2D 3-fold interpenetrated network<sup>19</sup> structure (Fig. 8) connected by a Hopf link, which is nothing but a [2]-catenane.<sup>2,20</sup>

Crystallization of **1** from  $\text{CH}_3\text{NO}_2$  with a trace amount of added  $\text{CF}_3\text{CH}_2\text{OH}$  ( $\text{CH}_3\text{NO}_2 : \text{CF}_3\text{CH}_2\text{OH} \sim 50 : 1$ ) afforded the  $1\cdot(\text{CH}_3\text{NO}_2)_2$  solvate as plate-shaped crystals with the space group *Pbca*. Four molecules of **1** are connected *via* solvent molecules to form an idealized (6,3) net of  $18.6 \times 13.3 \times 10.3$  Å cavities. The polycatenation of 2D hexagonal sheets completes the 3D crystal structure (Fig. 9). The network in this structure is different from that of the *PyzNO* cocrystal. This structure is an example of 2D  $\rightarrow$  3D polycatenation with a degree of catenation ( $\text{DOC}$ )<sup>2</sup> =  $2/2$ , which means that two layers are catenated with one hexagonal ring and *vice versa*. The  $\text{CH}_3\text{NO}_2$  solvate of **1** is identical to its *MeOH* and *EtOH* solvates<sup>5</sup> in terms of stoichiometry, space group, lattice parameters, catenation mode and the role of the solvent as bridges between the host molecules.

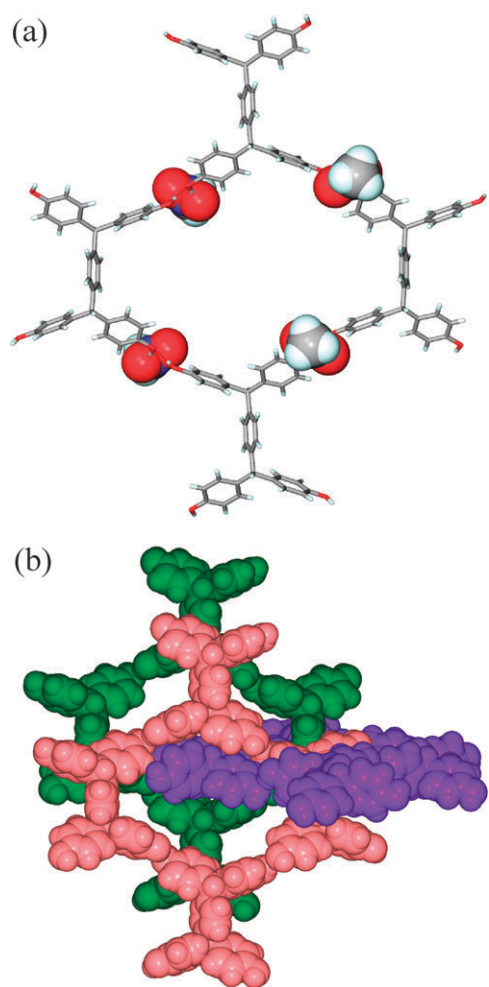
The use of  $\text{CH}_3\text{NO}_2$  as a minor component in the solvent mixture ( $\text{CH}_3\text{NO}_2 : \text{CF}_3\text{CH}_2\text{OH} \sim 1 : 6$ ) gave a solvated polymorph of  $1\cdot(\text{CH}_3\text{NO}_2)_2$  with the space group *P2<sub>1</sub>/c*. The asymmetric unit contains 0.5 host molecules and 1 guest molecule in both crystal structures. The network in this latter monoclinic form is best understood by analyzing the octamethyl derivative **4** $\cdot(\text{CHCl}_3)_2$  solvate.<sup>12</sup> Two host molecules hydrogen bond *via* an  $\text{O}-\text{H}\cdots\text{O}$  tetramer to form pentagons of  $5.4 \times 5.4$  Å that are occupied by the guest species (Fig. 10(a)). The 2D sheet of pentagonal ( $5_3^4$ ) nets in the (100) plane has four- and three-connected nodes in a 1 : 2 ratio.<sup>21</sup> This structure and the related  $1\cdot(\text{CH}_3\text{NO}_2)_2$  solvate (Fig. 10(b)) are early examples of all-organic pentagonal nets. A side-on approach of two H-shaped molecules (Fig. S4, ESI†) gives a pentagonal tiling of ( $5_3^4$ ) nets (Fig. 10(c)), such that the  $\text{sp}^3$  tetrahedral



**Fig. 8** (a) The  $\text{O}-\text{H}\cdots\text{O}$  hydrogen-bonded (6,3) network of expanded hexagonal rings (green lines show ring sides 1–6) in  $1\cdot(\text{PyzNO})_2$ . (b) The triply interpenetrated network connected by a Hopf link.

centers are 3-connected nodes and the 4-connected hydrogen bond tetramer is auto-generated (Fig. 10(d)). A tetrahedral center can function as a pseudo-trigonal or pseudo-square node (Fig. S5, ESI†).<sup>21a</sup> A difference between Catalan and the previously described hexagonal and ladder nets is that the present case is a uniform network topology (only one type *n*-gon) under the subclass of Catalan net (two nodes having different 3- and 4-connectivities), whereas the earlier examples were Platonic nets (all nodes are 3-connected).<sup>1a</sup>

Cocrystallization of **1** with quinoxaline afforded single crystals of  $1\cdot(\text{Quinox})_2$ , which were solved into the monoclinic space group *P2<sub>1</sub>/c*. The network structure is of the 1D polyrotaxane or polythreading type.<sup>16</sup> Distinct motifs can be entangled *via* rotaxane-like mechanical links, and this implies the presence of closed loops, as well as connectors that thread through the loops. However, in contrast to bimolecular rotaxanes, in which the loop and thread are made up from different molecules, here the loop and thread belong to the same binary molecular system (Fig. 11). The OH groups at the V-nodes of different H-shaped molecules orient convergently to form a closed loop (ring) with the co-former spacer, while the *para*-substituted benzene ring connects the loops (thread), as shown



**Fig. 9** (a)  $\text{CH}_3\text{NO}_2$  molecules act as bridges in the supramolecular hexagon of four H-shaped molecules in  $1 \cdot (\text{CH}_3\text{NO}_2)_2$  (*Pbca* form). (b)  $2\text{D} \rightarrow 3\text{D}$  polycatenation with a  $\text{DOC} = 2/2$  of the  $18.6 \times 13.3 \times 10.3$  Å cavity completing the molecular packing by space filling. The three sides of the pseudo-hexagon have different dimensions.

in Fig. 11(b) and (c). This polyrotaxane type of  $1\text{D} \rightarrow 1\text{D}$  polythreaded network of alternating rings and rods can be considered as “Euclidean entanglement”<sup>2</sup>, *i.e.* there is no increase in the dimensionality of the network.

The thermal behavior of the solvates is summarized in Table 3 and DSC/TGA plots are shown in Fig. S6 (ESI†).

## Discussion

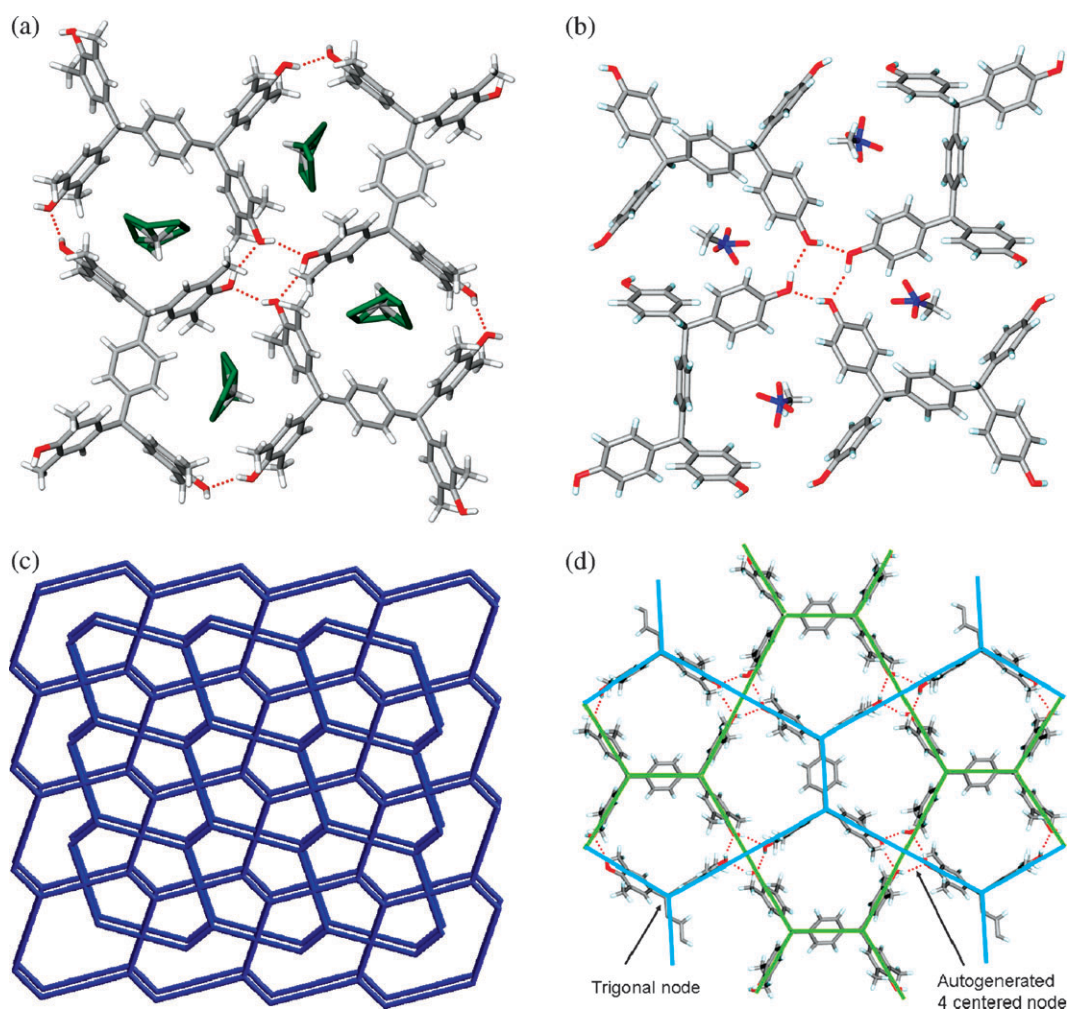
Solvents having only hydrogen bond acceptor groups, such as EtOAc, DMSO, dioxane and  $\text{CH}_3\text{CN}$ , generally result in a ladder network in their inclusion complexes with **1**. The phenol OH groups hydrogen bond to form 1D ladders and unused OH groups of the host molecule are hydrogen-bonded to the solvent acceptor, except in DMSO solvates. Because of its better acceptor strength, DMSO behaves as a double hydrogen bond acceptor and is part of the 1D ladder network. These small solvent molecules reside above and below the rectangular rung regions of host ladders. When bulky methyl or methoxy groups are present (as in **2** and **4**), even DMSO cannot come sufficiently close to the host to accept two

hydrogen bonds, perhaps for steric reasons. DMSO behaves as a single acceptor, similar to EtOAc, in these structures (Fig. S2, ESI†). Dioxane connects host ladders *via* hydrogen bonds. Solvents devoid of donor or acceptor groups generally occupy the channel or rung region of the host ladder by space filling, *e.g.* as in **4** (toluene). The pentagonal Catalan net in  $4 \cdot (\text{CHCl}_3)_2$  and  $1 \cdot (\text{CH}_3\text{NO}_2)_2$  came as an unexpected bonus.<sup>12</sup> This result was rationalized as the self-assembly of two H-shaped molecules in a side-on manner, which is a novel way of building a pentagonal ( $5_3^3$ ) net and is unprecedented compared to the two previous literature reports.<sup>21</sup> The larger volume of  $\text{CHCl}_3$  compared to  $\text{CH}_3\text{NO}_2$  means that the latter is present as a dimer in ladders, whereas the former solvent has one molecule in the cavity of **4**. Small sized solvent molecules, such as MeOH and EtOH, generally form hexagonal sheet structures through hydrogen bonding with the solvent. The large supramolecular hexagon ring achieves close packing through catenation or interpenetration.

In the case of heteroaromatic cocrystal formers,  $\pi$ -stacking plays an important role. Aromatic stacking is facilitated in the larger surface area rings of phenazine and quinoxaline, but not for 4,4'-bipyridine or its *N*-oxide, as seen in the crystal structures of  $1 \cdot (\text{Phez})_{1.5}$  and  $1 \cdot (\text{Quinox})_2$ . The ability of extended  $\pi$ -stacking to direct phenol OH groups towards convergent hydrogen bonding with aza heterocycles has been noted in cocrystal systems.<sup>22</sup> The  $\pi$ -stacking of quinoxaline is with a longer interplanar separation than phenazine, which results in a new kind of polythreading or polyrotaxane network. Co-formers with two hydrogen bond acceptor groups, such as 4,4'-bipyridine, usually act as connectors to give expanded ladders, *e.g.*  $1 \cdot (4,4'\text{-Bipy})_2$ . However, 4,4'-bipyridine-*N,N'*-dioxide behaves differently to give a distorted 2D net because hydrogen bond donors can approach the stronger N–O acceptor from many directions (in-plane and out-of-plane), whereas donor groups lie mostly in the aromatic plane of the pyridyl N acceptor, *i.e.* co-former functionality directs network variability.

Aoyama's group<sup>6</sup> illustrated organic zeolites constructed from tetraphenol **5**. Zeolites are a class of porous materials capable of sorbing guest molecules in pores or cavities. The guest molecules reside in internal cavities, which may be constructed by using intermolecular interactions such as hydrogen bonds and metal coordination bonds. Pentagonal and hexagonal channels and cavities can easily include a variety of solvent molecules. TGA showed that solvent molecules were released at their boiling point or at a slightly higher temperature in host–guest solvates of **1** and **4**. The host is stable up to  $\sim 260$  °C.

The different molecular networks analyzed in the 23 crystal structures of H-shaped tectons (13 new examples and 10 previously reported<sup>5,12</sup>) are summarized in Table 2 and shown in Fig. 12. Whereas such a large number of diverse network architectures are not unprecedented in metal–organic structures and coordination polymers,<sup>23</sup> organic networks are not as widespread. We reason that differences in hydrogen bonding and  $\pi$ -stacking due to the guest and co-former species are responsible for network diversity in conformationally-flexible H-shaped molecules. The molecular conformations of parent molecule **1** and octamethyl derivative **4**, both of which



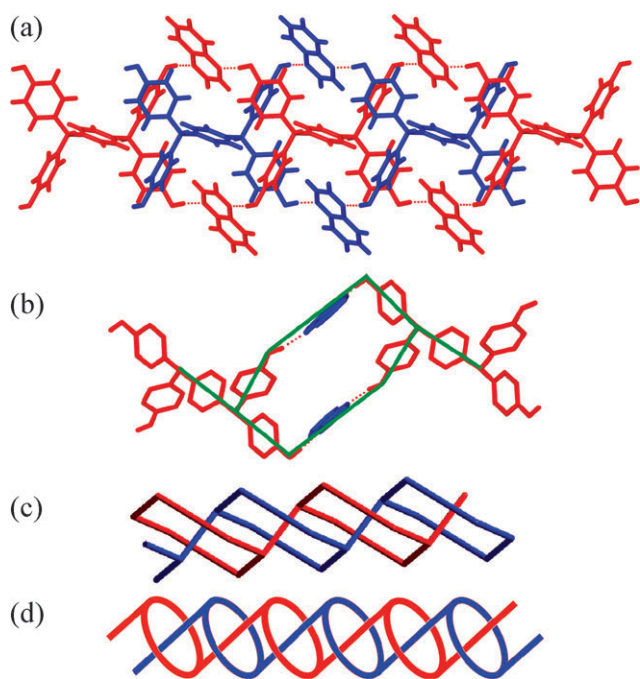
**Fig. 10** Pentagons of self-assembled **4** are filled with (a) disordered  $\text{CHCl}_3$  and (b)  $\text{CH}_3\text{NO}_2$  molecules in the monoclinic form of  $\mathbf{1}\cdot(\text{CH}_3\text{NO}_2)_2$ . (c) The 2D Catalan  $(5_4^3)$  net of H-shaped molecule **4** creates channels by the perfect stacking of sheets. (d) The side-on hydrogen bonding of H-shaped molecules *via* an  $\text{O}\cdots\text{H}\cdots\text{O}$  tetramer. Connection of the trigonal carbon centers auto-generates the 4-connected node.

crystallized in many solvates and guest-free forms, are shown in Fig. 13. Even though the phenol hydroxyl groups and *para*-phenyl ring adopt numerous orientations and conformations, the H-shape of these tetraphenol molecules and their coplanarity with respect to the mean plane defined in Fig. 1 is a persistent structural element. The phenol O and tetrahedral C atoms deviate by no more than 1 Å from the mean plane (Table S1, ESI<sup>†</sup>). It is clear that conformational flexibility, the orientation of the OH groups and solvent hydrogen bonding promote network diversity in H-shaped tectons. The relationship between the composition of the host network and the  $\text{p}K_{\text{a}}$  of co-former was recently discussed.<sup>24</sup> In general, however, predicting the topology and entanglement in organic 2D and 3D network structures is difficult,<sup>25</sup> and the most one can do is to rationalize the results after crystal structure determination and analysis.

## Conclusions

H-shaped host molecules **1–4** are quite remarkable in their guest inclusion and cocrystal-forming behavior, giving numerous

and diverse networks from the same starting tecton. Among 1D ladders and polyrotaxanes, 2D honeycomb and Catalan nets, as well as their interpenetrated/catenated structures, the most novel and remarkable results are the Catalan  $(5_4^3)$  nets in  $\mathbf{4}\cdot(\text{CHCl}_3)_2$  and  $\mathbf{1}\cdot(\text{CH}_3\text{NO}_2)_2$ , the two-component polyrotaxane of  $\mathbf{1}\cdot(\text{Quinox})_2$ , and the interpenetrated ladders in the  $\mathbf{1}\cdot(\text{Phez})_{1,5}$  cocrystal and its guest-free form. We have also shown novel examples of interpenetrated ladders, DOC 2/2 catenation, 2- and 3-fold interpenetrated  $(6,3)$  nets, and polythreaded rotaxanes. This structural diversity is a result of changes in guest hydrogen bonding,  $\pi$ -stacking and host molecular conformation. A reason for guest- or co-former-induced supramolecular diversity is that the H-shaped molecule is flexible in three ways—by the phenol OH group orientation, at the tetrahedral V-shaped bis(phenol) and at the *para*-phenyl connector. The presence of a second aromatic component gives interplay between hydrogen bonding and  $\pi$ -stacking motifs. The rational construction of novel network architectures from H-shaped molecules should be possible based on a better understanding of the network diversity of these structures.



**Fig. 11** (a) Chair cyclohexane rings in the **1**-(Quinox)<sub>2</sub> cocrystal structure sustained by O–H···N hydrogen bonds. (b) The V-shaped phenol OH groups are inwardly oriented by aromatic co-former  $\pi$ -stacking to form a ring, while the *para*-phenyl connector of **1** is the thread in the (c) 1D polyrotaxane network. (d) An idealized polyrotaxane.

## Experimental section

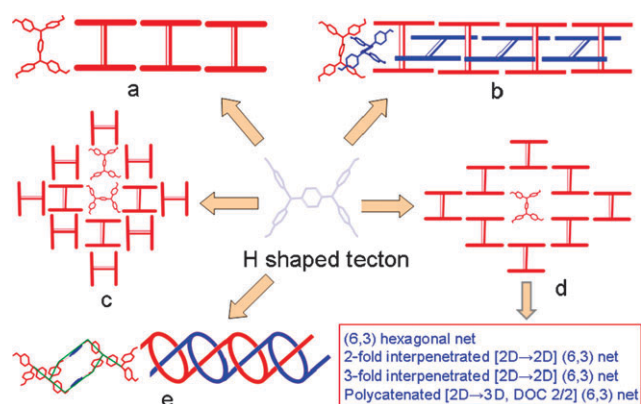
### Synthesis of host molecules

A mixture of terephthaldehyde (500 mg, 3.7 mmol) and phenol (1.8 mL, 14.9 mmol, 4 equiv.) in glacial acetic acid (10 mL) was treated dropwise with concentrated HCl (10 mL). The reaction mixture was stirred at room temperature for 24 h, poured onto

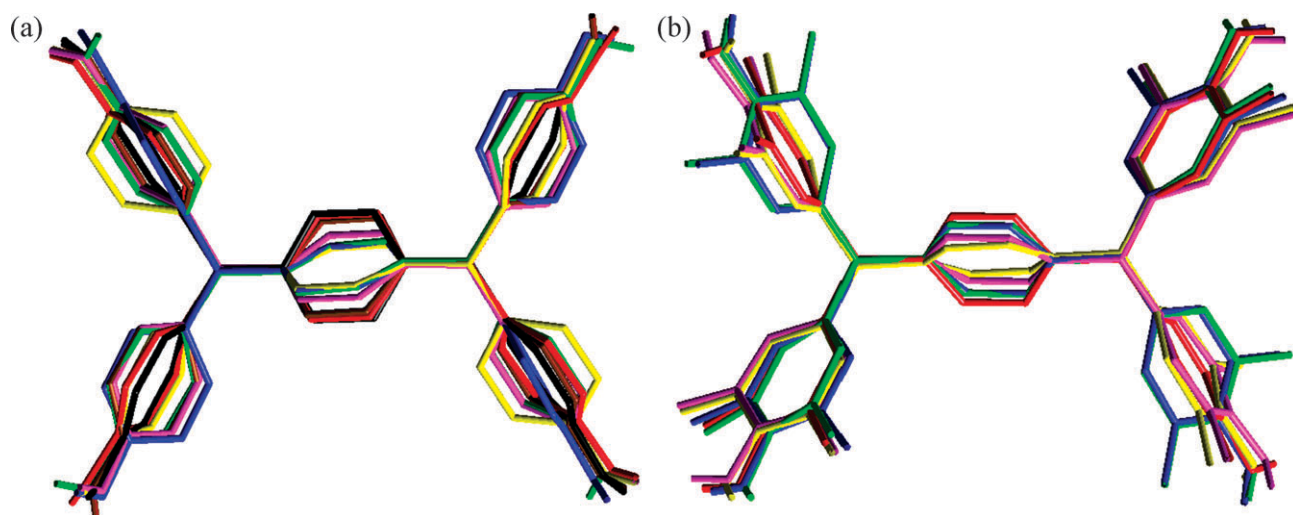
**Table 3** Thermal analysis (TGA and DSC) of the inclusion compounds

Inclusion complex <sup>a</sup>	Observed weight loss from TGA (%)	Calculated weight loss from host guest ratio in X-ray structure (%)	Guest release $T_{on}/^{\circ}\text{C}$ (from DSC)	Boiling point of the guest/ $^{\circ}\text{C}$
<b>1</b> ·(DMSO) <sub>2</sub>	28.9	24.8	153.7	189
<b>1</b> ·(CH <sub>3</sub> NO <sub>2</sub> ) <sub>2</sub> ( <i>Pbca</i> form)	20.3	20.5	96.8	100–103
<b>1</b> ·(EtOAc) <sub>2</sub>	26.2	27.1	90.0	77
<b>4</b> ·(DMSO) <sub>2</sub>	28.1	21.0	153.1	189
<b>4</b> ·(CH <sub>3</sub> NO <sub>2</sub> ) <sub>2</sub>	14.0	17.2	60.4	100–103
<b>4</b> ·(toluene)	16.1	13.6	125.0	110.6
<b>4</b> ·(CHCl <sub>3</sub> ) <sub>2</sub>	23.1	28.9	94.3	61.2

<sup>a</sup> The *P2<sub>1</sub>/c* form of the **1**·(CH<sub>3</sub>NO<sub>2</sub>)<sub>2</sub> and **1**·(i-PrOH)<sub>4</sub> samples could not be generated in sufficient quantity to undertake TGA. They exhibited  $T_{on}$  values in DSC at 108 and 78/113 °C, respectively.



**Fig. 12** Supramolecular networks in host-guest compounds and cocrystals of H-shaped molecules: (a) 1D ladder, (b) interpenetrated ladders, (c) Catalan or (5<sub>4</sub>) net, (d) common (6,3) hexagonal or 2D brick wall motif, and (e) polyrotaxane or polythreading.



**Fig. 13** The conformation of the H-shaped molecules in the crystal structures. (a) **1** in guest-free form having molecule A (red) and B (green), CH<sub>3</sub>NO<sub>2</sub> solvate (*Pbca* form) (blue), CH<sub>3</sub>NO<sub>2</sub> solvate (*P2<sub>1</sub>/c* form) (magenta), DMSO solvate (yellow), EtOAc solvate (brown), and i-PrOH solvate (black). (b) **4** in guest-free form (green), CHCl<sub>3</sub> solvate (red), CH<sub>3</sub>NO<sub>2</sub> solvate (blue), DMSO solvate (yellow) and toluene solvate (magenta). The H-shaped molecules adopt different conformations at the Y junction, as well as different *para*-phenyl connector and OH donor orientations, in each crystal structure. Only the H atoms of the phenol OH group are shown; the CH hydrogens are excluded for clarity.

crushed ice, and the precipitate filtered and washed with cold water. Dried compound **1** was purified by column chromatography using EtOAc–n-hexane (1 : 4) to yield 884 mg (50%) of the pure product.

Octamethoxy, tetramethyl and octamethyl derivatives **2**, **3** and **4** were prepared by a similar method using appropriate starting materials.

All compounds were synthesized, purified and characterized by IR and NMR spectroscopy. FT-IR spectra were recorded on a Jasco 5300 spectrophotometer. NMR spectra were recorded on a Bruker Avance spectrometer at 400 MHz. NMR chemical shifts on the  $\delta$  scale (ppm) and  $J$  couplings (Hz) are reported. Melting points were recorded on a Fisher-Johns apparatus and confirmed by endotherm peaks by DSC (Fig. S6, ESI<sup>†</sup>).

**1,4-Di[bis(4'-hydroxyphenyl)methyl]benzene (1)**. IR (KBr/ $\text{cm}^{-1}$ ): 3366, 1599, 1446, 1371, 1224, 760 and 636;  $^1\text{H}$  NMR ( $\delta$ , DMSO- $d_6$ ): 5.28 (2H, s, methine-CH), 6.64 (8H, d,  $J = 8$  Hz,

Ph-CH), 6.85 (8H, d,  $J = 8$  Hz, Ph-CH), 6.97 (4H, s, Ar-CH) and 9.22 (4H, s, OH). mp 275–278 °C. Yield 50%.

**1,4-Di[bis(3'-hydroxy-2',4'-dimethoxyphenyl)methyl]benzene (2)**. IR (KBr/ $\text{cm}^{-1}$ ): 3420, 2937, 1616, 1242, 1089, 783 and 694;  $^1\text{H}$  NMR ( $\delta$ ,  $\text{CDCl}_3$ ): 3.59 (12H, s,  $\text{OCH}_3$ ), 3.84 (12H, s,  $\text{OCH}_3$ ), 5.46 (4H, s, OH), 6.06 (2H, s, methine-CH), 6.31 (4H, d,  $J = 8$  Hz, Ph-CH), 6.50 (4H, d,  $J = 8$  Hz, Ph-CH) and 6.99 (4H, br s, Ar-CH). mp 249–251 °C. Yield 60%.

**1,4-Di[bis(4'-hydroxy-3'-methylphenyl)methyl]benzene (3)**. IR (KBr/ $\text{cm}^{-1}$ ): 3468, 2922, 1608, 1454, 1271, 775 and 609;  $^1\text{H}$  NMR ( $\text{CDCl}_3$ , DMSO- $d_6$ ): 2.50 (12H, s,  $\text{CH}_3$ ), 5.60 (2H, s, methine-CH), 7.05 (4H, s, Ar-CH), 7.07 (4H, s, Ph-CH), 7.18 (4H, s, Ph-CH), 7.33 (4H, s, Ph-CH) and 8.79 (4H, s, OH). mp 254–257 °C. Yield 55%.

**1,4-Di[bis(4'-hydroxy-3',5'-dimethylphenyl)methyl]benzene (4)**. IR (KBr/ $\text{cm}^{-1}$ ): 3586, 2918, 1670, 1302, 1147, 760 and 694;  $^1\text{H}$  NMR ( $\text{CDCl}_3$ ): 2.17 (24H, s,  $\text{CH}_3$ ), 4.48 (4H, s, OH), 5.25

**Table 4** Crystallographic data

	<b>1</b> (guest-free)	<b>1</b> -(EtOAc) <sub>2</sub>	<b>1</b> -(DMSO) <sub>2</sub>	<b>1</b> -(i-PrOH) <sub>4</sub>	<b>1</b> -(Phez) <sub>1.5</sub>	<b>1</b> -(Quinox) <sub>2</sub>	<b>1</b> -(PyzNO) <sub>2</sub>	<b>1</b> -(4,4'-BipyNO) <sub>2</sub>
Chemical formula	C <sub>32</sub> H <sub>26</sub> O <sub>4</sub>	C <sub>40</sub> H <sub>42</sub> O <sub>8</sub>	C <sub>36</sub> H <sub>38</sub> O <sub>6</sub> S <sub>2</sub>	C <sub>44</sub> H <sub>58</sub> O <sub>8</sub>	C <sub>50</sub> H <sub>38</sub> N <sub>3</sub> O <sub>4</sub>	C <sub>48</sub> H <sub>38</sub> N <sub>4</sub> O <sub>4</sub>	C <sub>40</sub> H <sub>34</sub> N <sub>4</sub> O <sub>8</sub>	C <sub>52</sub> H <sub>42</sub> N <sub>4</sub> O <sub>8</sub>
Formula weight	474.53	650.74	630.78	714.90	744.83	734.82	698.71	850.90
Crystal system	Triclinic	Triclinic	Monoclinic	Monoclinic	Triclinic	Monoclinic	Monoclinic	Orthorhombic
Space group	<i>P</i> $\bar{1}$	<i>P</i> $\bar{1}$	<i>P</i> 2 <sub>1</sub> / <i>c</i>	<i>C</i> 2/ <i>c</i>	<i>P</i> $\bar{1}$	<i>P</i> 2 <sub>1</sub> / <i>c</i>	<i>P</i> 2 <sub>1</sub> / <i>c</i>	<i>Pca</i> 2 <sub>1</sub>
<i>T</i> /K	100	100	100	100	298	298	298	298
<i>a</i> /Å	10.1926(10)	7.3791(5)	11.0387(11)	33.506(3)	10.2976(8)	14.472(6)	13.064(2)	20.631(4)
<i>b</i> /Å	11.0478(10)	10.4359(8)	7.4017(7)	5.8797(4)	11.2084(9)	16.115(6)	7.6296(11)	7.1465(14)
<i>c</i> /Å	13.0960(14)	11.3692(8)	19.4980(19)	22.036(2)	18.4225(15)	8.057(3)	16.929(3)	28.309(5)
$\alpha$ (°)	101.849(2)	93.3570(10)	90	90	96.0410(10)	90	90	90
$\beta$ (°)	102.082(2)	95.2410(10)	96.343(2)	115.061(2)	103.7210(10)	93.044(7)	99.722(2)	90
$\gamma$ (°)	115.675(2)	100.8240(10)	90	90	102.7000(10)	90	90	90
<i>Z</i>	2	1	2	4	2	2	2	4
<i>V</i> /Å <sup>3</sup>	1224.1(2)	853.77(11)	1583.3(3)	3932.5(6)	1987.1(3)	1876.3(13)	1663.1(4)	4173.9(14)
<i>D</i> <sub>c</sub> /g cm <sup>-3</sup>	1.287	1.266	1.323	1.207	1.245	1.301	1.395	1.354
$\mu$ /mm <sup>-1</sup>	0.084	0.087	0.214	0.082	0.079	0.084	0.099	0.092
Reflections collected	12394	7902	15752	19346	20835	11675	16408	40681
Observed reflections	2595	3008	2273	2668	4071	2287	2750	5879
Total reflections	4633	3323	3127	3880	7790	3678	3273	8317
<i>R</i> <sub>1</sub> ( <i>I</i> > 2 $\sigma$ ( <i>I</i> ))	0.0786	0.0401	0.0603	0.0759	0.0651	0.0829	0.0599	0.1249
w <i>R</i> <sub>2</sub> (all)	0.1032	0.1049	0.1273	0.2116	0.1538	0.1429	0.1334	0.2726
Goodness-of-fit	0.991	1.048	1.062	1.042	1.016	1.118	1.141	1.112

	<b>2</b> -(DMSO) <sub>2</sub>	<b>2</b> -(dioxane) <sub>2</sub>	<b>3</b> -(DMF) <sub>2</sub>	<b>3</b> -(CH <sub>3</sub> NO <sub>2</sub> ) <sub>2</sub>	<b>4</b> (guest-free)	<b>4</b> -(toluene)	<b>4</b> -(DMSO) <sub>2</sub>
Chemical formula	C <sub>44</sub> H <sub>54</sub> O <sub>14</sub> S <sub>2</sub>	C <sub>48</sub> H <sub>58</sub> O <sub>16</sub>	C <sub>42</sub> H <sub>48</sub> N <sub>2</sub> O <sub>6</sub>	C <sub>38</sub> H <sub>40</sub> N <sub>2</sub> O <sub>8</sub>	C <sub>40</sub> H <sub>42</sub> O <sub>4</sub>	C <sub>47</sub> H <sub>50</sub> O <sub>4</sub>	C <sub>44</sub> H <sub>54</sub> O <sub>6</sub> S <sub>2</sub>
Formula weight	870.99	890.94	676.82	652.72	586.74	678.87	742.99
Crystal system	Monoclinic	Triclinic	Monoclinic	Triclinic	Monoclinic	Triclinic	Monoclinic
Space group	<i>P</i> 2 <sub>1</sub> / <i>c</i>	<i>P</i> $\bar{1}$	<i>C</i> 2/ <i>c</i>	<i>P</i> $\bar{1}$	<i>P</i> 2 <sub>1</sub> / <i>c</i>	<i>P</i> $\bar{1}$	<i>P</i> 2 <sub>1</sub> / <i>n</i>
<i>T</i> /K	100	298	100	298	100	100	298
<i>a</i> /Å	10.8550(7)	9.039(4)	23.799(2)	5.5173(5)	15.0090(17)	8.7313(7)	11.340(2)
<i>b</i> /Å	14.2040(9)	10.605(4)	8.0974(8)	12.0094(12)	5.5072(6)	10.2761(9)	8.2249(15)
<i>c</i> /Å	14.8984(9)	13.461(6)	18.3595(15)	12.9806(13)	18.887(2)	11.4745(10)	21.892(4)
$\alpha$ (°)	90	101.940(7)	90	91.144(2)	90	64.9820(10)	90
$\beta$ (°)	111.1700(10)	98.428(8)	113.226(5)	96.446(2)	104.850(2)	75.9800(10)	102.049(4)
$\gamma$ (°)	90	112.198(7)	90	91.410(2)	90	86.5800(10)	90
<i>Z</i>	2	1	4	1	2	1	2
<i>V</i> /Å <sup>3</sup>	2142.1(2)	1132.4(8)	3251.3(5)	854.17(14)	1509.0(3)	904.07(13)	1996.9(6)
<i>D</i> <sub>c</sub> /g cm <sup>-3</sup>	1.350	1.307	1.383	1.269	1.291	1.247	1.236
$\mu$ /mm <sup>-1</sup>	0.192	0.098	0.092	0.089	0.082	0.078	0.180
Reflections collected	21901	11616	11912	8866	14825	9481	19868
Observed reflections	3017	2046	1923	2165	2260	2754	2287
Total reflections	4227	4379	3202	3331	2970	3553	3891
<i>R</i> <sub>1</sub> ( <i>I</i> > 2 $\sigma$ ( <i>I</i> ))	0.0641	0.0751	0.0670	0.0594	0.0604	0.0764	0.1189
w <i>R</i> <sub>2</sub> (all)	0.1565	0.1797	0.1694	0.1388	0.1338	0.1760	0.1888
Goodness-of-fit	1.000	0.990	0.978	1.023	1.042	1.074	1.181

(2H, s, methine-CH), 6.70 (8H, s, Ph-CH) and 6.99 (4H, s, Ar-CH). 261–264 °C. Yield 60%.

### X-Ray crystallography

Reflections were collected on a Bruker SMART CCD diffractometer. Mo-K $\alpha$  ( $\lambda = 0.71073 \text{ \AA}$ ) radiation was used to collect the X-ray reflections of all the crystals (1–4). Data reduction was performed using Bruker SAINT software.<sup>26</sup> Structures were solved and refined using SHELXL-97<sup>27</sup> with anisotropic displacement parameters for non-H atoms. Hydrogen atoms on O were experimentally located in all of the crystal structures. All C–H atoms were fixed geometrically. A check of the final CIF file using PLATON<sup>28</sup> did not show any missed symmetry. Disordered solvent molecules in 1-(i-PrOH)<sub>4</sub> (one out of two) and 3-(DMF)<sub>2</sub> were removed by SQUEEZE within PLATON. The crystal structures of 1-(Phez)<sub>1,5</sub> and 1-(4,4'-BipyNO)<sub>2</sub> could only be solved satisfactorily after fixing the hydroxyl H atoms in refinement cycles (HFIX 83 command). Friedel pairs were averaged in case of the non-centrosymmetric space group *Pca*2<sub>1</sub> for 1-(4,4'-BipyNO)<sub>2</sub> (MERC 4 command). All hydrogen atoms were fixed (HFIX command) and toluene disorder was modelled with isotropic refinement for 1-(toluene). CIF files of all the crystal structures contain refinement details under `_refine_special_details`. The crystallographic parameters for the 1–4 structures are summarized in Table 4. Hydrogen bond distances listed in Table 1 are neutron-normalized to fix the donor–H distance to its accurate neutron value in the X-ray crystal structures (O–H 0.983 Å, N–H 1.009 Å, C–H 1.083 Å). The  $T_{\min}$  and  $T_{\max}$  values were derived from SHELX based on the crystal size, since the absorption correction is minimal in these light atom-containing crystal structures. Packing diagrams were prepared using X-Seed.<sup>29†</sup>

### Acknowledgements

We thank the CSIR (01(2079)/06/EMR-II) and DST (SR/S1/RFOC-01/2007 Ramanna Fellowship) for research funding. R. T. and B. S. thank the UGC and CSIR for fellowships. DST (IRPHA) funded the CCD X-ray diffractometer and the UGC is thanked for the UPE program. We thank a crystallographic reviewer for hints regarding an improved structure solution for the disordered guest species and a chemical referee for valuable insight into interpenetrated network modes.

### References

- (a) A. F. Wells, *Three-Dimensional Nets and Polyhedra*, Wiley, New York, 1977; (b) M. O'Keeffe and B. G. Hyde, *Philos. Trans. R. Soc. London, Ser. A*, 1980, **295**, 553; (c) S. R. Batten and R. Robson, *Angew. Chem., Int. Ed.*, 1998, **37**, 1460; (d) G. R. Desiraju, *Chem. Commun.*, 1997, 1475; (e) B. Moulton and M. J. Zaworotko, *Chem. Rev.*, 2001, **101**, 1629; (f) G. R. Desiraju, *J. Mol. Struct.*, 2003, **656**, 5; (g) K. Biradha, M. Sarkar and L. Rajput, *Chem. Commun.*, 2006, 4169; (h) L. Öhrström and K. Larsson, *Molecule-Based Materials*, Elsevier, Amsterdam, 2005; (i) N. Malek, T. Maris, M.-É. Perron and J. D. Wuest, *Angew. Chem., Int. Ed.*, 2005, **44**, 4021; (j) R. Bishop, *Acc. Chem. Res.*, 2009, **42**, 67.
- (a) L. Carlucci, G. Ciani and D. M. Proserpio, *Coord. Chem. Rev.*, 2003, **246**, 247; (b) L. Carlucci, G. Ciani and D. M. Proserpio, *CrystEngComm*, 2003, **5**, 269; (c) S. R. Batten, *CrystEngComm*, 2001, **3**, 67.
- (a) L. Carlucci, G. Ciani and D. M. Proserpio, *Chem. Commun.*, 2004, 380; (b) L. Carlucci, G. Ciani, S. Maggini and D. M. Proserpio, *Cryst. Growth Des.*, 2008, **8**, 162.
- (a) I. A. Baburin, V. A. Blatov, L. Carlucci, G. Ciani and D. M. Proserpio, *Cryst. Growth Des.*, 2008, **8**, 519; (b) I. A. Baburin and V. A. Blatov, *Acta Crystallogr., Sect. B: Struct. Sci.*, 2007, **63**, 791.
- S. Aitipamula and A. Nangia, *Supramol. Chem.*, 2005, **17**, 17.
- (a) K. Endo, T. Sawaki, M. Koyanagi, K. Kobayashi, H. Masuda and Y. Aoyama, *J. Am. Chem. Soc.*, 1995, **117**, 8341; (b) T. Tanaka, T. Tasaki and Y. Aoyama, *J. Am. Chem. Soc.*, 2002, **124**, 12453; (c) K. Endo, T. Koike, T. Sawaki, O. Hayashida, H. Masuda and Y. Aoyama, *J. Am. Chem. Soc.*, 1997, **119**, 4117; (d) Y. Aoyama, K. Endo, T. Anzai, Y. Yamaguchi, T. Sawaki, K. Kobayashi, N. Kanehisa, H. Hashimoto, Y. Kai and H. Masuda, *J. Am. Chem. Soc.*, 1996, **118**, 5562; (e) K. Tanaka, K. Endo and Y. Aoyama, *Chem. Lett.*, 1999, 887; (f) Y. Aoyama, K. Endo, K. Kobayashi and H. Masuda, *Supramol. Chem.*, 1994, **4**, 229.
- (a) S. Aitipamula and A. Nangia, *Chem.–Eur. J.*, 2005, **11**, 6727; (b) V. S. Senthil Kumar, A. Nangia, M. T. Kirchner and R. Boese, *New J. Chem.*, 2003, **27**, 224.
- G. R. Swiegers and T. J. Malefetse, *Chem. Rev.*, 2000, **100**, 3483.
- (a) P. Grosshans, A. Jouaiti, N. Kardouh, M. W. Hosseini and N. Kyritsakas, *New J. Chem.*, 2003, **27**, 1806; (b) F. G. Klärner and B. Kahlert, *Acc. Chem. Res.*, 2003, **36**, 919; (c) M. Harmata, *Acc. Chem. Res.*, 2004, **37**, 862; (d) A. Sygula, F. R. Fronczek, R. Sygula, P. W. Rabideau and M. M. Olmstead, *J. Am. Chem. Soc.*, 2007, **129**, 3842.
- (a) S. L. James, *Chem. Soc. Rev.*, 2003, **32**, 276; (b) K. Biradha, *CrystEngComm*, 2003, **5**, 374; (c) S. A. Barnett and N. R. Champness, *Coord. Chem. Rev.*, 2003, **246**, 145; (d) S. Kitagawa, R. Kitaura and S. Noro, *Angew. Chem., Int. Ed.*, 2004, **43**, 2334; (e) N. W. Ockwig, O. Delgado-Friedrichs, M. O'Keeffe and O. M. Yaghi, *Acc. Chem. Res.*, 2005, **38**, 176; (f) S. Kitagawa and K. Uemura, *Chem. Soc. Rev.*, 2005, **34**, 109.
- (a) J.-S. Yang and J.-L. Yan, *Chem. Commun.*, 2008, 1501; (b) M. A. Alvarez, I. Amor, M. E. García and M. A. Ruiz, *Inorg. Chem.*, 2008, **47**, 7963.
- R. Thakuria, B. Sarma and A. Nangia, *Cryst. Growth Des.*, 2008, **8**, 1471.
- A. D. Bond, *CrystEngComm*, 2007, **9**, 833.
- (a) V. T. Nguyen, P. D. Ahn, R. Bishop, M. L. Scudder and D. C. Craig, *Eur. J. Org. Chem.*, 2001, 4489; (b) X.-Q. Lü, M. Pan, J.-R. He, Y.-P. Cai, B.-S. Kang and C.-Y. Su, *CrystEngComm*, 2006, **8**, 827; (c) V. S. Senthil Kumar, F. C. Pigge and N. P. Rath, *New J. Chem.*, 2003, **27**, 1554; (d) A. D. Bond, *Chem.–Eur. J.*, 2004, **10**, 1885.
- (a) B. K. Saha, R. K. R. Jetti, L. S. Reddy, S. Aitipamula and A. Nangia, *Cryst. Growth Des.*, 2005, **5**, 887; (b) B. R. Bhogala and A. Nangia, *New J. Chem.*, 2008, **32**, 800.
- (a) D. Whang and K. Kim, *J. Am. Chem. Soc.*, 1997, **119**, 451; (b) C. S. A. Fraser, M. C. Jennings and R. J. Puddephatt, *Chem. Commun.*, 2001, 1310; (c) L. Carlucci, G. Ciani and D. M. Proserpio, *Cryst. Growth Des.*, 2005, **5**, 37; (d) K. K. Arora and V. R. Pedireddi, *Cryst. Growth Des.*, 2005, **5**, 1309; (e) A. A. Salaudeen, C. A. Kilner and M. A. Halcrow, *Chem. Commun.*, 2008, 5200; (f) X.-Y. Cao, Q.-P. Lin, Y. Y. Qin, J. Zhang, Z.-J. Li, J.-K. Cheng and Y.-G. Yao, *Cryst. Growth Des.*, 2009, **9**, 20.
- C. Laurence and M. Berthelot, *Perspect. Drug Discovery Des.*, 2000, **18**, 39.
- (a) B. Sarma, S. Roy and A. Nangia, *Chem. Commun.*, 2006, 4918; (b) S. Aitipamula, G. R. Desiraju, M. Jaskólski, A. Nangia and R. Thaimattam, *CrystEngComm*, 2003, **5**, 447; (c) H.-J. Lehmler, L. W. Robertson, S. Parkin and C. P. Brock, *Acta Crystallogr., Sect. B: Struct. Sci.*, 2001, **58**, 140; (d) C. P. Brock, *Acta Crystallogr., Sect. B: Struct. Sci.*, 2002, **58**, 1025.
- (a) B. R. Bhogala, P. Vishweshwar and A. Nangia, *Cryst. Growth Des.*, 2002, **2**, 325; (b) T. R. Shattock, P. Vishweshwar, Z. Wang and M. J. Zaworotko, *Cryst. Growth Des.*, 2005, **5**, 2046; (c) Q.-Y. Yang, S.-R. Zheng, R. Yang, M. Pan, R. Cao and C.-Y. Su, *CrystEngComm*, 2009, **11**, 680.

- 20 (a) J.-P. Sauvage, *Acc. Chem. Res.*, 1998, **31**, 611; (b) S. S.-Y. Chui, R. Chen and C.-M. Che, *Angew. Chem., Int. Ed.*, 2006, **45**, 1621; (c) S. T. Caldwell, G. Cooke, B. Fitzpatrick, D.-L. Long, G. Rabania and V. M. Rotello, *Chem. Commun.*, 2008, 5912; (d) J.-Q. Liu, Y.-Y. Wang, L.-F. Ma, G.-L. Wen, Q.-Z. Shi, S. R. Batten and D. M. Proserpio, *CrystEngComm*, 2008, **10**, 1123.
- 21 (a) B. Moulton, J. Lu and M. J. Zaworotko, *J. Am. Chem. Soc.*, 2001, **123**, 9224; (b) S. W. Keller and S. Lopez, *J. Am. Chem. Soc.*, 1999, **121**, 6306.
- 22 (a) B. Sarma, L. S. Reddy and A. Nangia, *Cryst. Growth Des.*, 2008, **8**, 4546; (b) L. R. MacGillivray, J. L. Reid and J. A. Ripmeester, *J. Am. Chem. Soc.*, 2000, **122**, 7817; (c) T. Frišičić and L. R. MacGillivray, *Chem. Commun.*, 2005, 5748; (d) G. S. Papaefstathiou, Z. Zhong, L. Geng and L. R. MacGillivray, *J. Am. Chem. Soc.*, 2004, **126**, 9158; (e) L. R. MacGillivray, G. S. Papaefstathiou, T. Frišičić, T. D. Hamilton, D.-K. Bučar, Q. Chu, D. B. Varshney and I. G. Georgiev, *Acc. Chem. Res.*, 2008, **41**, 280.
- 23 (a) A. J. Blake, N. R. Champness, P. Hubberstey, W.-S. Li, M. A. Withersby and M. Schröder, *Coord. Chem. Rev.*, 1999, **183**, 117; (b) L. Carlucci, G. Ciani, D. M. Proserpio and S. Rizzato, *J. Solid State Chem.*, 2000, **152**, 211; (c) D. K. Kumar, D. A. Jose, A. Das and P. Dastidar, *Inorg. Chem.*, 2005, **44**, 6933; (d) M. R. Montney, S. M. Krishnan, N. M. Patel, R. M. Supkowski and R. L. LaDuca, *Cryst. Growth Des.*, 2007, **7**, 1145; (e) X.-Q. Liang, X.-H. Zhou, C. Chen, H.-P. Xiao, Y.-Z. Li, J.-L. Zuo and X.-Z. You, *Cryst. Growth Des.*, 2009, **9**, 1041; (f) Z. Su, J. Xu, J. Fan, D.-J. Liu, Q. Chu, M.-S. Chen, S.-S. Chen, G.-X. Liu, X.-F. Wang and W.-Y. Sun, *Cryst. Growth Des.*, 2009, **9**, 2801.
- 24 A. Delori, E. Suresh and V. R. Pedireddi, *Chem.–Eur. J.*, 2008, **14**, 6967.
- 25 Y.-B. Men, J. Sun, Z.-T. Huang and Q.-Y. Zheng, *Angew. Chem., Int. Ed.*, 2009, **48**, 2873.
- 26 G. M. Sheldrick, *SADABS, Program for area detector adsorption correction*, Institute for Inorganic Chemistry, University of Göttingen, Germany, 1996.
- 27 (a) G. M. Sheldrick, *SHELXS-97, Program for the solution of crystal structures*, University of Göttingen, Germany, 1997; (b) G. M. Sheldrick, *SHELXL-97, Program for the refinement of crystal structures*, University of Göttingen, Germany, 1997.
- 28 (a) A. L. Spek, *PLATON, A Multipurpose Crystallographic Tool*, Utrecht University, Utrecht, The Netherlands, 2002; (b) A. L. Spek, *J. Appl. Crystallogr.*, 2003, **36**, 7.
- 29 L. J. Barbour, *X-Seed: Graphical Interface to SHELX-97 and POV-Ray*, University of Missouri-Columbia, Columbia, MO, 1999.